

Measurements of fluence profiles in femtosecond laser filaments in air

XIAO-LONG LIU,^{1,2} WEIBO CHENG,¹ MASSIMO PETRARCA,³ AND PAVEL POLYNKIN^{1,*}

¹College of Optical Sciences, University of Arizona, 1630 East University Boulevard, Tucson, Arizona 85721, USA

²Academy of Opto-Electronics, Chinese Academy of Science, Beijing 100094, China

³La Sapienza University, SBAI Department, via A. Scarpa 14, 00161 Rome, Italy

*Corresponding author: ppolynkin@optics.arizona.edu

Received 29 August 2016; accepted 16 September 2016; posted 21 September 2016 (Doc. ID 274592); published 10 October 2016

We introduce a technique to measure fluence distributions in femtosecond laser beams with peak intensity of up to several hundred terawatts per square centimeter. Our approach is based on the dependence of single-shot laser ablation threshold for gold on the angle of incidence of the laser beam on the gold sample. We apply this technique to the profiling of fluence distributions in femtosecond laser filaments at a wavelength of 800 nm in air. The peak intensity is found to be clamped at a level that depends on the external beam focusing. The limiting value of the peak intensity attainable in long-range 800 nm air filaments, under very loose focusing conditions (f -number above ~ 500), is about 55 TW/cm². © 2016 Optical Society of America

OCIS codes: (140.3330) Laser damage; (140.3295) Laser beam characterization; (010.1300) Atmospheric propagation; (190.5940) Self-action effects.

<http://dx.doi.org/10.1364/OL.41.004751>

The conventional approach to the absolute measurement of a fluence distribution in an intense laser beam is based on the reduction of the beam power, by a large fraction, through one or several consecutive reflections of the beam off an uncoated dielectric surface. Then the fluence distribution in the original beam can be obtained by multiplying the fluence distribution in the low-power replica beam by the known power-reduction factor. This simple approach becomes impractical once the peak fluence of the laser beam exceeds the ablation threshold fluence for the sampling surface, which, in the case of femtosecond and picosecond laser pulses at near-infrared laser wavelengths, is of the order of one Joule per square centimeter for common dielectric surfaces illuminated at normal incidence [1].

In a recent article [2], we quantified the dependence of the threshold fluence for single-shot laser ablation, on the angle of incidence (AOI) of the laser beam on the sample. Those experiments were conducted with three types of common optical materials: a metal (gold), a dielectric (soda-lime glass), and a semiconductor (silicon).

The ablation threshold fluence versus the AOI of the laser beam for a gold surface ablated with an S-polarized

femtosecond laser beam is shown in Fig. 1. The parameters of the laser pulse are specified in the figure caption. The experimental procedure used to obtain these data is discussed in detail in [2]. Note that the data shown in Fig. 1 are for the peak threshold fluence. Some researchers choose to specify threshold fluence averaged over the cross-section of the beam [3]. For a Gaussian beam profile, the average fluence equals one half of the peak fluence. Also note that in the case shown, the ablation threshold fluence grows with the AOI, about twice as fast as the simple law $\propto 1/\cos$ (AOI), which would be expected from the argument based on the spreading of the laser energy over a larger surface of the sample, as the AOI is increased. As discussed in [2], the growth of the threshold fluence with AOI is such that the laser fluence transmitted into the material, at the point of ablation threshold, remains constant, independent of the AOI. Here, we utilize the dependence of the ablation threshold fluence on the AOI for profiling intense femtosecond laser beams propagating in air in the filamentation regime.

In femtosecond laser filamentation in air [4,5], the self-focusing of the intense laser beam with peak power on the order

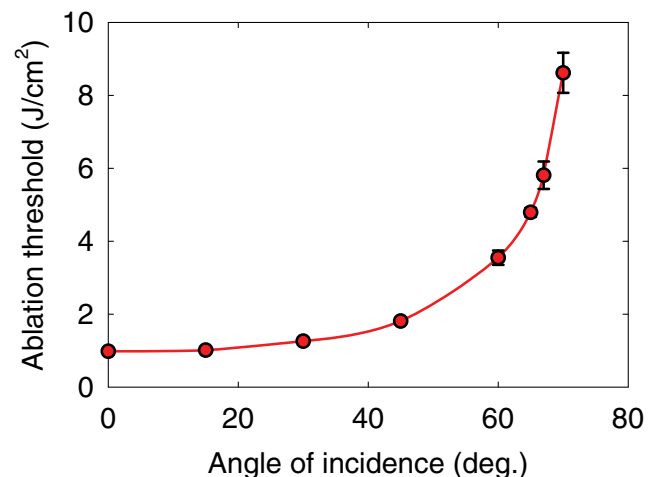


Fig. 1. Data for the single-shot ablation threshold fluence for a gold surface in air, at different AOIs of the S-polarized laser beam on the sample [2]. The incident laser pulse at 800 nm center wavelength has 60 fs FWHM duration.

of 10 GW and above, drives a transverse beam collapse on propagation. The collapse is stopped and dynamically counterbalanced by air ionization and the associated nonlinear absorption and de-focusing. This dynamic balance limits (or clamps) the value of the peak laser intensity attainable in laser filaments. Knowing the absolute value of the clamping intensity is important for understanding and quantifying the physical mechanisms involved in various phenomena that accompany laser filamentation, such as supercontinuum generation [6], strong-field ionization [7], THz generation [8], and air lasing [9].

Numerical values for the peak intensity in femtosecond laser filaments in air that have been reported over the years range from 30 TW/cm² to about 150 TW/cm² [10–15]. Laser pulses at 800 nm center wavelength and durations in the range from 30 to 200 fs have been used in most of the prior studies. The variability of the reported values for the peak intensity is due to the differences in both the experimental conditions and the measurement techniques used in the above-cited works.

In our experiments, we generate laser filaments by focusing a laser beam at a wavelength of 800 nm in the laboratory air with a spherical mirror telescope. The effective focal length of the telescope is adjustable so that the ratio of the focal length to the input beam diameter (f -number) can be varied from 80 (“tight” focusing) to 1600 (“loose” focusing). The duration of the incident laser pulse is 47 fs, the maximum pulse energy is 2.5 mJ, and the pulse repetition rate is 10 Hz. The transverse profile of the laser beam at the output from the laser is very close to a Gaussian. Under all experimental conditions that we use, a single filament is formed within the transverse beam profile. The absence of multi-filamentation is evident from the appearance of the single-shot ablation craters produced by the filament on a gold-coated silicon wafer.

In order to measure the optical fluence profile in the femtosecond filament, we produce single-shot ablations by the filament on a gold surface at different AOIs. Our sample is a 1000 Å-thick gold layer deposited onto a silicon wafer, which is the same type of sample that we used to collect the data shown in Fig. 1. The duration of the laser pulse used to collect that data was approximately 10 fs different from what we use in the experiments on filament profiling reported here. That difference does not affect our measurements, as the ablation threshold fluence is weakly dependent on pulse duration for pulses shorter than about 1 ps [1]. The sample is mounted on a manual rotation stage, allowing the AOI of the filament beam on the surface of the sample to be varied. The practical range of the AOI is from 0° (normal incidence) to about 75°. The polarization of the laser beam is perpendicular to the plane of incidence (S-polarization). The manual rotation stage, with the sample attached to it, is mounted on a motorized linear translation stage, which enables ablation in the single-shot regime. The resulting single-shot ablation craters produced by the filament, at a particular position along the beam-propagation path, are subsequently inspected with a microscope. At each particular value of the AOI, the boundary of the ablation crater marks the line-out of the fluence profile of the laser beam, at the fluence level equal to the ablation threshold fluence corresponding to that AOI. The fact that the incident laser fluence on the beam axis can significantly exceed the ablation threshold fluence, resulting in the onset of thermal effects in ablation [16], is of no importance here, because we are only interested

in the appearance of the boundary of the ablation crater, where fluence is exactly at the level of the single-shot ablation threshold. In the case of a single air filament, the fluence profile is very close to axial symmetry, but the above mapping procedure can be applied to beams with arbitrarily shaped cross-sections.

By definition, we introduce a quantity equal to the ratio of fluence to the initial FWHM duration of the laser pulse and multiplied by a factor of 0.94. So defined, peak intensity is a function of propagation distance and the transverse coordinates within the beam profile. It is representative of the peak optical intensity in the filament, provided that the temporal shape and FWHM duration of the assumed to be Gaussian laser pulse do not appreciably change on the nonlinear propagation in air. The latter assumption has been supported by numerical simulations [17–19], with the exception of the ultra-fast sub-cycle temporal spikes that have been shown to form on the trailing edge of the pulse; those temporal spikes carry only a very small fraction of the total beam power [20].

We point out that our experimental procedure only rigorously maps the distribution of fluence, not intensity. The corresponding distribution of intensity, derived from the measured distribution of fluence according to the above definition, is only an approximation, as we do not account for the complex temporal reshaping of the laser pulse on propagation. At the same time, the fluence mapping will be accurate even in the case of strong temporal reshaping of the laser pulse, because ablation threshold fluence is weakly dependent on pulse duration, as long as the pulse remains sub-picosecond [1].

With the following data, we show the peak intensity defined according to the above postulative definition, in which the average intensity equals fluence divided by the constant input FWHM pulse duration and multiplied by the 0.94.

In Fig. 2, we show data for the peak intensity on the beam axis, as a function of the propagation distance, for the case when a 2 mJ, 47 fs laser pulse with 6 mm input beam diameter is focused by a spherical mirror telescope with an effective focal length of 3.7 m. These focusing conditions correspond to the

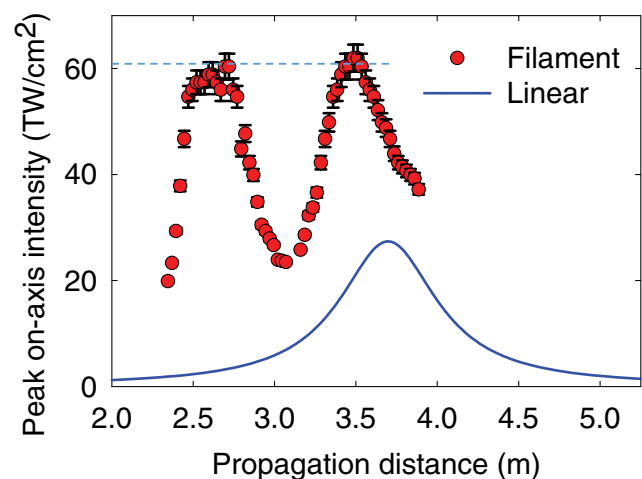


Fig. 2. Data for the peak intensity, versus propagation distance, for the air filament produced by a 2 mJ, 47 fs laser pulse at 800 nm. The laser beam is weakly externally focused by a spherical mirror telescope with the f -number $f_{\#} = 616$. The solid line shows a calculated value of the peak intensity for linear propagation of the beam, with the maximum at the position of the linear focus of the mirror telescope.

effective f -number of $f_{\#} = 616$. The peak intensity was determined by producing a single-shot ablation on a gold surface at the AOI that was gradually increased to the point when ablation was no longer observed. At that point, the peak fluence on the axis of the filament was equal to the ablation threshold fluence for gold at that AOI. The experimental errors shown are due to the $\pm 0.1^{\circ}$ accuracy of the manual rotation stage and the associated uncertainty of the value of the AOI of the laser filament on the gold sample. From the measured data, two focusing-defocusing cycles are evident, with the maximum intensity clamped at about 60 TW/cm^2 in both cycles. The calculated peak intensity for the case of linear propagation, under the same focusing conditions, is shown with a solid line.

Experimental data obtained under different focusing conditions show the same trend: the peak intensity on the beam axis undergoes consecutive focusing-defocusing cycles along the propagation direction, while the maximum intensity in each cycle is limited (clamped) at the certain level, which is specific to the particular linear focusing conditions used. These conclusions are consistent with the earlier reports [21,22].

In Fig. 3, we show data for the transverse intensity profile in the laser filament, at the propagation distance where the peak fluence reaches a maximum (the position of the first self-focusing collapse). The three profiles shown correspond to three different values of the input pulse energy, as indicated in the figure legend. The f -number of the external linear focusing system equals 616 in all three cases. Note that depending on the pulse energy, the self-focusing collapse occurs at different positions along the propagation path. Specifically, the collapse points corresponding to the input pulse energies of 1.5 mJ, 2.0 mJ, and 2.5 mJ are 3.045 m, 2.720 m, and 2.445 m, respectively.

It is evident from the data that, as the input pulse energy is increased, the peak intensity on the axis of the filament remains relatively unchanged, supporting the familiar intensity clamping concept. At the same time, the filament blooms, and the diameter of the filament grows by about 20%, corresponding to the increase of the cross-sectional area by about 44%, as the

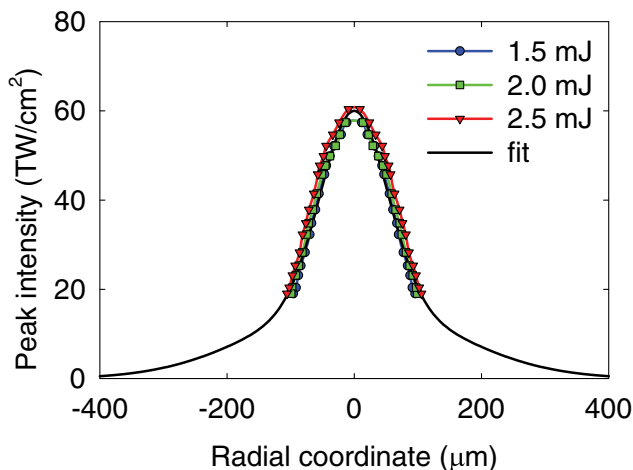


Fig. 3. Data for intensity profiles in femtosecond laser filaments in air, for the case of external beam focusing with f -number $f_{\#} = 616$, at different values of the laser pulse energy. The beam profiles are measured at the longitudinal position where the peak fluence reaches a maximum (the position of the self-focusing collapse).

laser pulse energy increases from 1.5 mJ to 2.5 mJ (which is about a 67% increase). These observations contradict the prevalent notion that the core of the filament that results from a self-similar, self-focusing beam collapse always carries one critical power [23]. The black solid line shows, for the case of input pulse energy of 2.5 mJ, the result of a calculation that partitions the total beam energy into two parts: the filament core, with the peak intensity and the FWHM beam size derived from the measurement data, and the remaining part that is linearly focused by the telescope system with a given input beam diameter and f -number.

In Fig. 4, we show the experimental data for the maximum on-axis intensity along the propagation direction versus f -number of the external focusing telescope system. As in Fig. 2, the experimental errors are due to the $\pm 0.1^{\circ}$ accuracy of the manual rotation stage. The maximum intensity attainable in the filament strongly depends on the external focusing conditions. For the case of very weak focusing, which corresponds to the values of the f -number above ~ 500 , the maximum intensity saturates at the level of 55 TW/cm^2 . This intensity level is representative of what can be achieved in the long-range femtosecond laser filaments at a wavelength of 800 nm in air. The corresponding values calculated for the case of linear focusing of a 2 mJ, 47 fs-long laser pulse are shown with a dark solid line. Under these conditions, the maximum intensity attainable through linear focusing in a vacuum equals that in the femtosecond filament in air, for the f -number of the external focusing system of about 375.

In summary, we have applied the dependence of ablation threshold fluence on the AOI of the laser beam on a gold surface, to profile fluence distributions in femtosecond laser filaments in air. In agreement with the previously published works, we found that the maximum fluence attainable in femtosecond air filaments is clamped, independently of the input pulse energy, at the level that strongly depends on the conditions of external linear focusing. Under the assumption of weak temporal reshaping of the laser pulse on propagation, the value for the clamping intensity in long-range laser filaments at 800 nm, derived from our measurements of fluence, is about 55 TW/cm^2 .

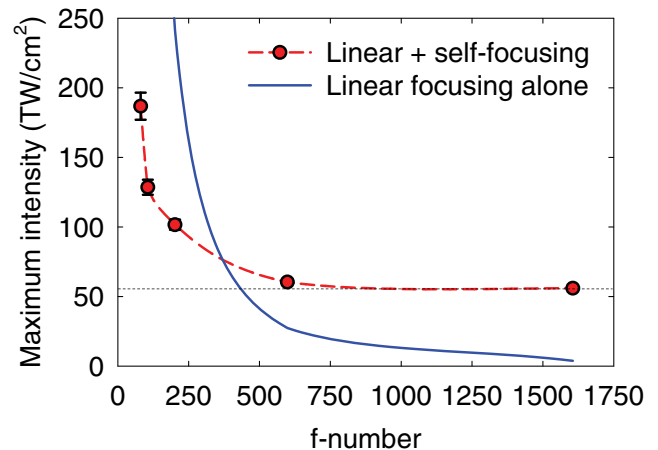


Fig. 4. Data for the maximum on-axis intensity along the propagation path, as a function of the f -number of the linear focusing optic. The results of a calculation of the peak intensity for a 2 mJ, 47 fs pulse are shown with a solid line.

Funding. Air Force Office of Scientific Research (AFOSR) (FA9550-12-1-0482, FA9550-16-1-0013); Defense Threat Reduction Agency (DTRA) (HDTRA 1-14-1-0009); National Natural Science Foundation of China (NSFC) (11404335).

Acknowledgment. We thank Dr. Thomas D. Milster and Mr. Lee Johnson for assistance with operation of the electron microscope and Dr. Ali Azarm for helpful discussions.

REFERENCES

1. B. C. Stuart, M. D. Feit, S. Herman, A. M. Rubenchik, B. W. Shore, and M. D. Perry, *J. Opt. Soc. Am. B* **13**, 459 (1996).
2. X. L. Liu, W. Cheng, M. Petrarca, and P. Polynkin, "Universal threshold for femtosecond laser ablation with oblique illumination," arXiv: 1608.05884 (2016).
3. A. Ben-Yakar and R. Byer, *J. Appl. Phys.* **96**, 5316 (2004).
4. A. Couairon and A. Mysyrowicz, *Phys. Rep.* **441**, 47 (2007).
5. L. Berge, S. Skupin, R. Nuter, J. Kasparian, and J. P. Wolf, *Rep. Prog. Phys.* **70**, 1633 (2007).
6. E. T. J. Nibbering, P. F. Curley, G. Grillon, B. S. Prade, M. A. Franco, F. Salin, and A. Mysyrowicz, *Opt. Lett.* **21**, 62 (1996).
7. H. Xu, Y. Cheng, S. L. Chin, and H. B. Sun, *Laser Photon. Rev.* **9**, 275 (2015).
8. C. D'Amico, A. Houard, M. Franco, B. Prade, and A. Mysyrowicz, *Phys. Rev. Lett.* **98**, 235002 (2007).
9. P. R. Hemmer, R. B. Miles, P. Polynkin, T. Siebert, A. V. Sokolov, P. Sprangle, and M. O. Scully, *Proc. Natl. Acad. Sci. USA* **108**, 3130 (2011).
10. J. Kasparian, R. Sauerbrey, and S. L. Chin, *Appl. Phys. B* **71**, 877 (2000).
11. P. P. Kiran, S. Bagchi, C. L. Arnold, S. R. Krishnan, G. R. Kumar, and A. Couairon, *Opt. Express* **18**, 21504 (2010).
12. J. F. Daigle, A. Jaroń-Becker, S. Hosseini, T. J. Wang, Y. Kamali, G. Roy, A. Becker, and S. L. Chin, *Phys. Rev. A* **82**, 023405 (2010).
13. S. Xu, X. Sun, B. Zeng, W. Chu, J. Zhao, W. Liu, Y. Cheng, Z. Xu, and S. L. Chin, *Opt. Express* **20**, 299 (2012).
14. T. Vockerodt, D. S. Steingrube, E. Schulz, M. Kretschmar, U. Morgner, and M. Kovacev, *Appl. Phys. B* **106**, 529 (2012).
15. S. I. Mityukovskiy, Y. Liu, A. Houard, and A. Mysyrowicz, *J. Phys. B* **48**, 094003 (2015).
16. S. Nolte, C. Momma, H. Jackobs, A. Tünnermann, B. N. Chichkov, B. Wellegehausen, and H. Welling, *J. Opt. Soc. Am. B* **14**, 2716 (1997).
17. A. Couairon and L. Bergé, *Phys. Rev. Lett.* **88**, 135003 (2002).
18. S. Champeaux and L. Bergé, *Phys. Rev. E* **71**, 046604 (2005).
19. S. Champeaux, L. Bergé, D. Gordon, A. Ting, J. Peñano, and P. Sprangle, *Phys. Rev. E* **77**, 036406 (2008).
20. M. B. Gaarde and A. Couairon, *Phys. Rev. Lett.* **103**, 043901 (2009).
21. O. G. Kosareva, W. Liu, N. A. Panov, J. Bernhardt, Z. Ji, M. Sharifi, R. Li, Z. Xu, J. Liu, Z. Wang, J. Ju, X. Lu, Y. Jiang, Y. Leng, X. Liang, V. P. Kandidov, and S. L. Chin, *Laser Phys.* **19**, 1776 (2009).
22. X. L. Liu, X. Lu, X. Liu, T. T. Xi, F. Liu, J. L. Ma, and J. Zhang, *Opt. Express* **18**, 26007 (2010).
23. J. V. Moloney, M. Kolesik, M. Mlejnek, and E. M. Wright, *Chaos* **10**, 559 (2000).